[redacted] [redacted]

224

Copy
RM E56C16

TECH LIBRARY KAFB, NM
0144084

NACA RM E56C16

6959

NACA

Reg # 14964

RESEARCH MEMORANDUM

EXPERIMENTAL INVESTIGATION OF INTERFERENCE EFFECTS OF LATERAL-SUPPORT STRUTS ON AFTERBODY PRESSURES AT MACH 1.9

By John L. Klann and Ronald G. Huff

Lewis Flight Propulsion Laboratory
Cleveland, Ohio

HADC
TECHNICAL LIBRARY
AFL 2811

[redacted]

[redacted]

NATIONAL ADVISORY COMMITTEE
FOR AERONAUTICS
WASHINGTON
May 14, 1956

[redacted]

[redacted]

Classification cancelled (or changed to UNCLASSIFIED)

By Authority of AFSC Tech Pub Announcement #146
(OFFICER AUTHORIZED TO CHANGE)

By ..... 2 May 58

(GRADE OF OFFICER MAKING CHANGE)

27 Mar 61
DATE

TECH LIBRARY KAFB, NM
0144084

NATIONAL ADVISORY COMMITTEE FOR AERONAUTICS

RESEARCH MEMORANDUM

EXPERIMENTAL INVESTIGATION OF INTERFERENCE EFFECTS OF LATERAL-SUPPORT STRUTS ON AFTERBODY PRESSURES AT MACH 1.9

By John L. Klann and Ronald G. Huff

4027

CQ-1

SUMMARY

A series of single and double unswept, lateral-support struts was tested at a Mach number of 1.9 on a cone-cylinder body at zero angle of attack. These struts consisted essentially of a rectangular box section with identical wedge fairings fore and aft. Wedge half-angles of 8° were used on struts with ratios of thickness to chord of 0.050, 0.070, and 0.100, while 4° half-angles were used on struts having a ratio of 0.047. The area of the rectangular part of the strut cross sections was held constant. Measurements included pressures over the body surface from the cone to, and including, the base.

All strut-body interference effects were small beyond a length of 8 body diameters. However, an oblique shock wave originating at the intersection of the strut leading-edge shock wave and the tunnel-wall boundary layer did affect afterbody pressures. This shock interference was alleviated by reducing the leading-wedge angle. No afterbody interference penalty was suffered by retaining a larger trailing-wedge angle.

INTRODUCTION

Wind-tunnel models for jet-exit research are commonly supported by lateral struts. The size of these struts is frequently determined by the duct passage area needed in the struts for the jet air supply rather than by structural requirements. Hence, the strut cross-sectional area and therefore the strut-body interference effects may often be quite large. This problem cannot, in general, be solved by simply lengthening the body to move the aft portion away from the interference region, since the jet exit must be kept upstream of tunnel-reflected shocks from the forebody and strut leading edge.

This investigation was conducted to determine experimentally the interference due to a specific configuration of body and struts. A cone-cylinder body was tested at zero angle of attack in the NACA Lewis

18- by 18-inch (Mach number 1.9) wind tunnel with a series of single and double unswept struts. Discussion is restricted to variations in the afterbody pressures due to the presence of support struts.

SYMBOLS

The following symbols are used in this report:

A area of rectangular part of strut cross section, 1.05 sq in. (see fig. 1)

C_p pressure coefficient, $\frac{p - p_0}{q_0}$

c strut chord, in.

D body diameter, 1.75 in.

L length of rectangular part of strut cross section, in.

l length of leading or trailing strut wedge, in.

p local static pressure

q dynamic pressure

t thickness of rectangular part of strut cross section, in.

x axial distance measured from body cone tip, in.

α strut wedge half-angle, deg

θ angular body coordinate measured clockwise from plane of struts, deg (see fig. 1)

Subscripts:

b base of cone-cylinder body

le leading edge of struts

0 free stream

4027

APPARATUS AND PROCEDURE

This test was conducted in the NACA Lewis 18- by 18-inch (Mach number 1.9) wind tunnel. The tunnel total temperature was 150° F and the Reynolds number was 3.2×10^6 per foot.

A series of single and double unswept struts was tested on a 20° cone-cylinder body having a length-to-diameter ratio of 12. Sketches and dimensions of the body and strut cross sections are shown in figure 1. Leading- and trailing-wedge half-angles of 8° were employed on the struts with thickness ratios (t/c) of 0.050, 0.070, and 0.100 (struts B, C, and D, respectively), while the struts having a thickness ratio of 0.047 (struts A) had half-angles of 4°. The area of the rectangular part (fig. 1) of the strut cross sections was held constant. The location of static-pressure orifices on the body surface is shown in table I.

4027

The cone-cylinder body was mounted in the tunnel with a cylindrical sting having a diameter of 0.508 body diameter (0.508D) and a length from the base of the body of 4 body diameters. Both single and double struts were mounted at zero angle of attack from the body to the tunnel walls and positioned on the body so that the leading side of the rectangular part of the strut cross sections was fixed longitudinally on the model ($x_{le} + l = 5.95$ in., a constant). Single struts were tested only at an angular body coordinate θ of 180°. A small wire ring was put on the body cone tip to initiate a turbulent boundary layer.

CQ-1 back

The model was manually alined with the tunnel centerline and checked, with the tunnel in operation, by four cone-surface static-pressure orifices 90° apart. The tunnel-air dewpoint was held at -5° F (or less) throughout the test. Pressures were photographed from multitube manometer boards, read to within 0.05 inch of tetrabromoethane and reduced to pressure coefficients. Two separate tests of the sting-mounted body with no struts indicated a reproducibility to within 0.005 of the pressure coefficients.

RESULTS AND DISCUSSION

A schematic sketch of shock-wave intersections is shown in figure 2. The conical shock wave from the cone tip (not shown in fig. 2), on reflection at the tunnel walls, intersected the sting support beyond the base of the body. The nonreflected oblique shocks 1 and 2 originated at the strut leading and trailing edges. A third nonreflected oblique shock wave (3 in fig. 2) arose from the thickened boundary layer immediately behind the intersection of the strut leading-edge shock with the tunnel wall.

[redacted]

Experimental pressure distributions on the cylindrical portion of the body surface are presented in figures 3 to 6. Approximate shock intersections on the body surface are indicated on the curves. The position of the intersection of shock wave 3 in the $\theta = 0^{\circ}$ distributions applies only to the double-strut curves. Since the single struts were mounted at $\theta = 180^{\circ}$, the similar intersection occurred, in this case, about 1.7 body diameters downstream of the shown intersection of shock wave 3.

Considering first the effects of strut-body interference and confining attention the afterbody, it is seen that, beyond a length of 8 body diameters, all pressure coefficients (except the double struts having a thickness ratio of 0.100) are within 0.02. These variations will be considered small. The configurations with the struts having thickness ratios of 0.047 and 0.050 (figs. 3 and 4), both single and double, exhibit the least spread from the model afterbody pressures. For all $\theta = 90^{\circ}$ distributions between shock waves 2 and 3, the single strut curves are closer to the no-strut body-pressure coefficients than the double-strut curves. However, in the $\theta = 0^{\circ}$ distributions between shock waves 2 and 3, the reverse is true. The circumferential-pressure distributions shown in figures 3 to 6 are consistent and indicate (excluding $x/D = 5.75$) no severe pressure gradients.

Any reduction of the support strut chord that does not add to the afterbody interference effects will increase the relatively interference-free and, therefore, workable length of afterbody on a jet-exiting model. From figures 3 and 4 it can be noted that there is no essential change in the distance required behind the strut trailing edges to recover (within any chosen pressure increment) to body-alone pressures between strut wedge half-angles of 4° and 8°. Hence, the use of a larger trailing-wedge angle has the advantage of reducing the total strut chord with these data indicating no associated afterbody interference penalty.

When the interference of the nonreflected shock wave 3 (fig. 2) is considered, pressure disturbances are clearly observed in the $\theta = 90^{\circ}$ curves (fig. 6) for a thickness ratio of 0.100 and in the double struts ($\theta = 0^{\circ}$ curves) with thickness ratios of 0.050, 0.070, and 0.100 (figs. 4 to 6). Since shock wave 3 intersected the model surface in the vicinity of the last pressure orifice for the 90° distributions of the struts having thickness ratios of 0.050 and 0.070 (figs. 4 and 5), only an incipient disturbance can be observed. The curves for the 4° half-angles (fig. 3) are particularly noticeable for lack of any adverse effect of this disturbance. One apparent means of alleviating the effects of this interfering shock is to use a smaller leading-wedge angle. Also, since this shock originates at the strut intersection with the tunnel wall, a downstream movement of this juncture may cause the shock wave to miss the body surface. Hence, sweeping struts back from the body is another possible solution to the problem of reducing the effects of this interfering shock wave.

Figure 7 presents the results of the base-pressure measurements. The sting lowered the general level of the base pressure slightly from the interference-free values of reference 1. The additional interference effect due to struts was apparent but very small. The interference was larger at $\theta = 0^{\circ}$ than at $\theta = 90^{\circ}$, while all pressure coefficients were within 0.015.

SUMMARY OF RESULTS

4027

This investigation of effects of lateral-support strut interference on the afterbody pressures of a 20° cone-cylinder model at Mach 1.9 has indicated the following:

1. Strut-body interference effects were small beyond lengths of 8 body diameters.

2. Afterbody pressure disturbances due to a nonreflected oblique shock wave originating at the intersection of the strut leading-edge shock wave with the tunnel-wall boundary layer were detected. This interference was alleviated by using a smaller leading-wedge angle.

3. No afterbody interference penalty was suffered by retaining a larger trailing-wedge angle.

Lewis Flight Propulsion Laboratory
National Advisory Committee for Aeronautics
Cleveland, Ohio, March 23, 1956

REFERENCE

1. Love, Eugene S.: A Summary of Information on Support Interference at Transonic and Supersonic Speeds. NACA RM L53K12, 1954.

TABLE I. - LOCATION OF STATIC-PRESSURE ORIFICES

ON CONE-CYLINDER SURFACE

Axial distance, x, in.	Angular body coordinate, θ, deg						
1.03	0						90
2.03	0						90
3.40	0	22.5		45		67.5	90
4.89	0	22.5		45		67.5	90
5.14	0	22.5		45		67.5	90
5.56							90
7.06							90
8.56							90
10.06				45		67.5	90
11.56							90
13.06							90
14.56	0	22.5		45		67.5	90
16.06	0						90
17.56	0						90
19.06	0						90
20.52		22.5		45		67.5	
Base	0		30		60		90

4027

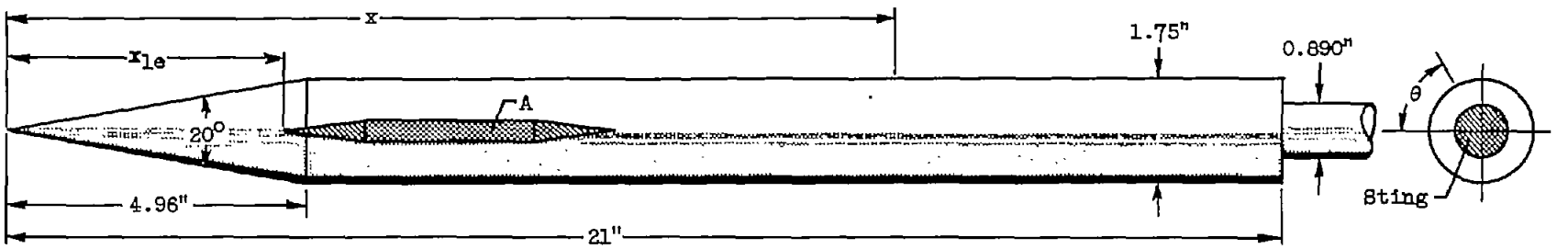

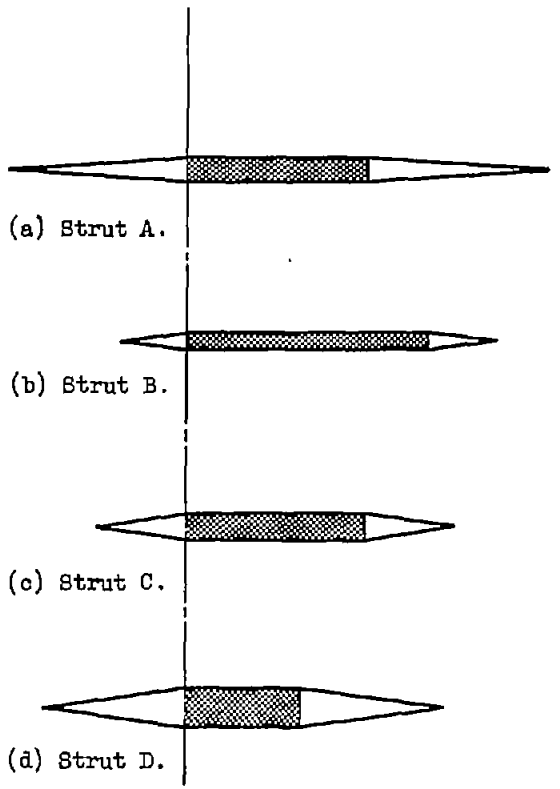

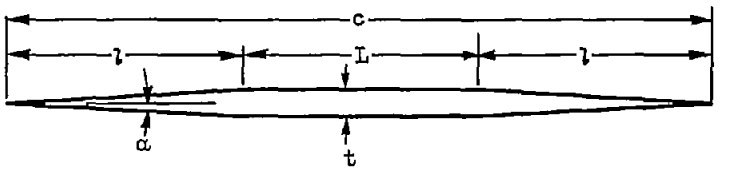

CD-5016

Strut	t/c	α, deg	L, in.	t, in.	c, in.	l, in.	x_{le}, in.
A	0.047	4	2.73	0.383	8.21	2.74	3.21
B	.050	8	3.67	.285	5.70	1.01	4.94
C	.070	8	2.73	.383	5.46	1.36	4.59
D	.100	8	1.74	.603	6.03	2.15	3.81

Figure 1. - Model and strut geometry.

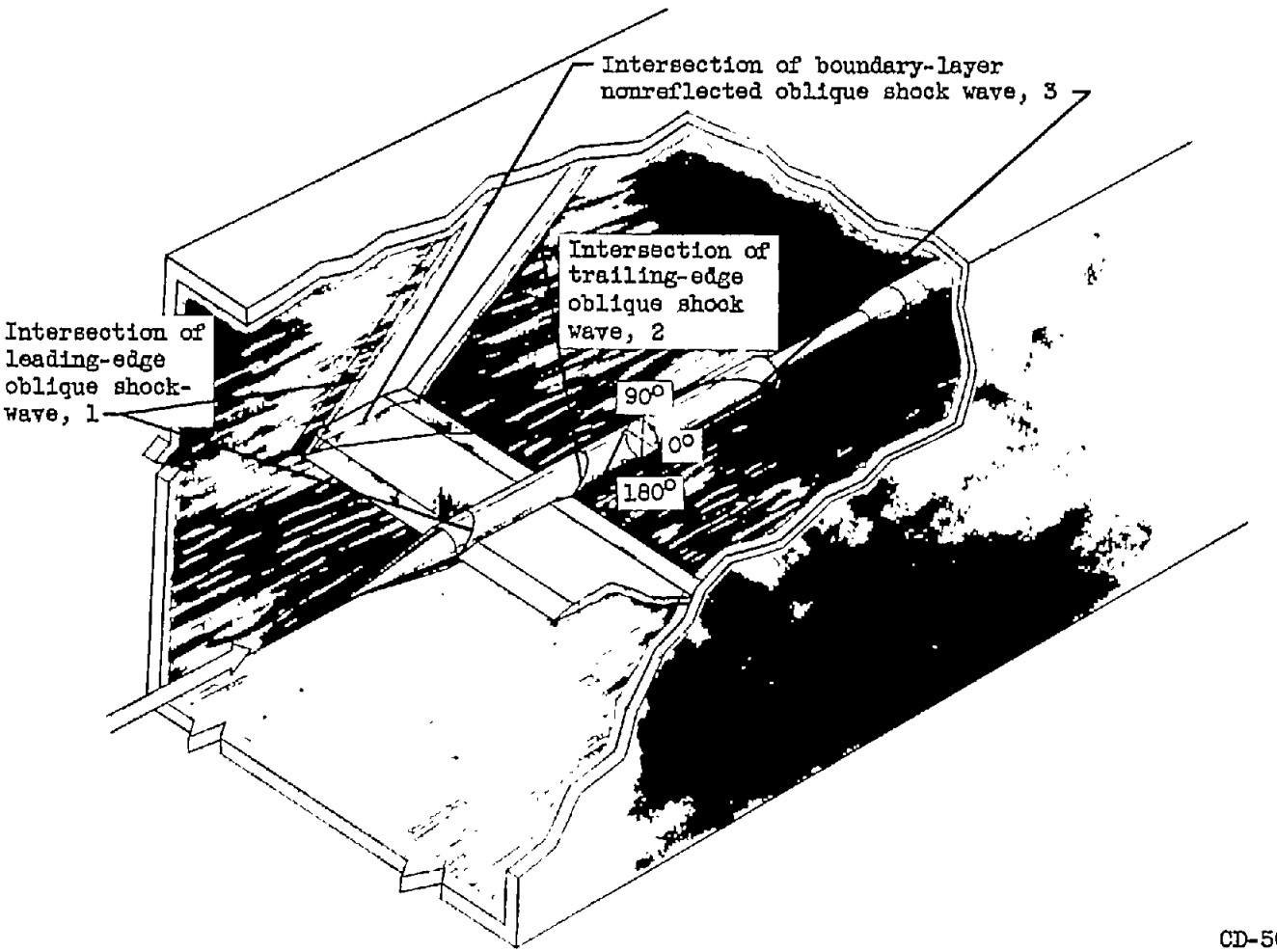

CD-5017

Figure 2. - Shock-wave intersections on model.

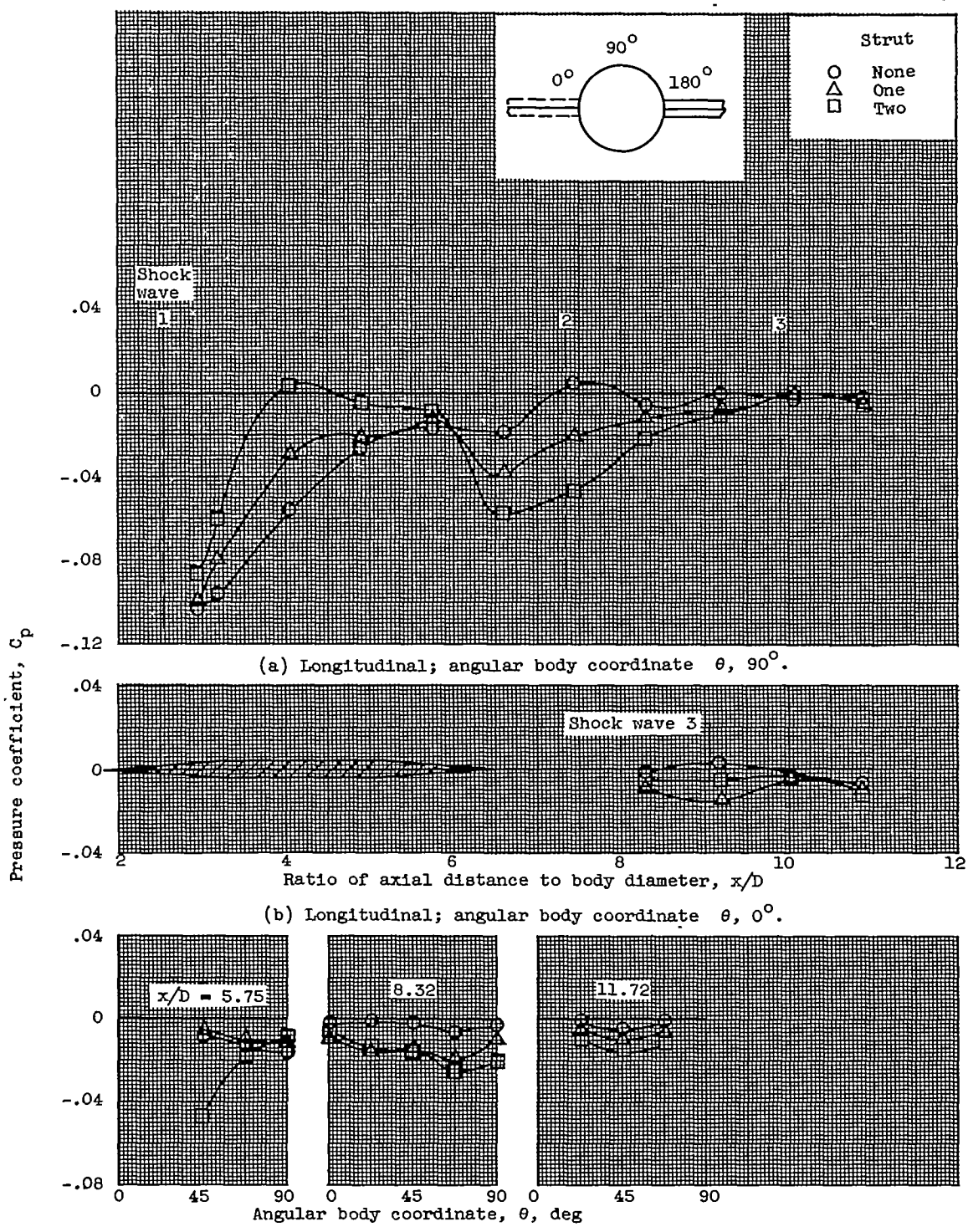

(c) Circumferential.

Figure 3. - Experimental body-pressure distributions for strut A (thickness ratio, 0.047; wedge half-angle, 4°).

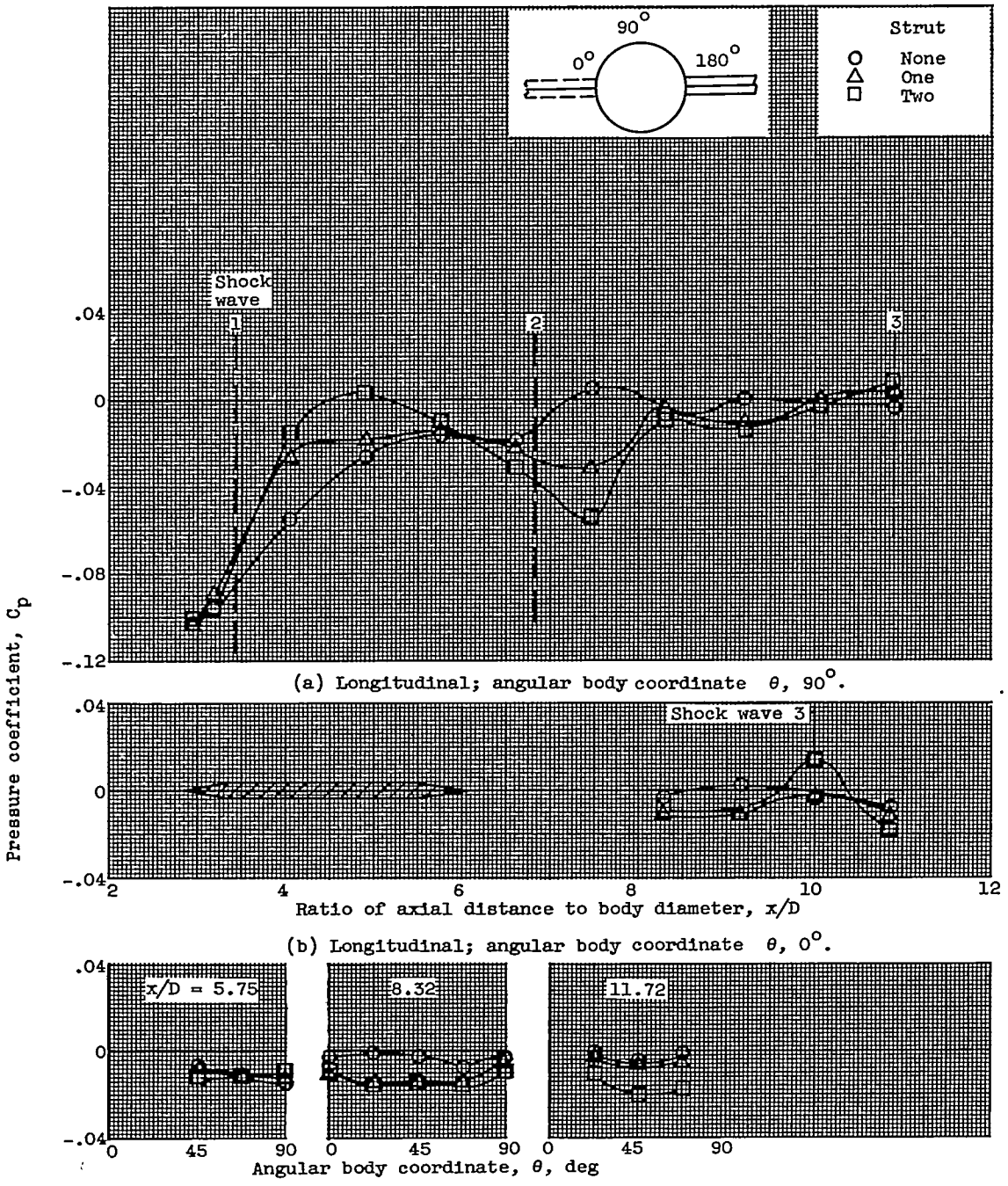

(a) Longitudinal; angular body coordinate θ, 90°.

(b) Longitudinal; angular body coordinate θ, 0°.

(c) Circumferential.

Figure 4. - Experimental body-pressure distribution for strut B (thickness ratio, 0.050; wedge half-angle, 8°).

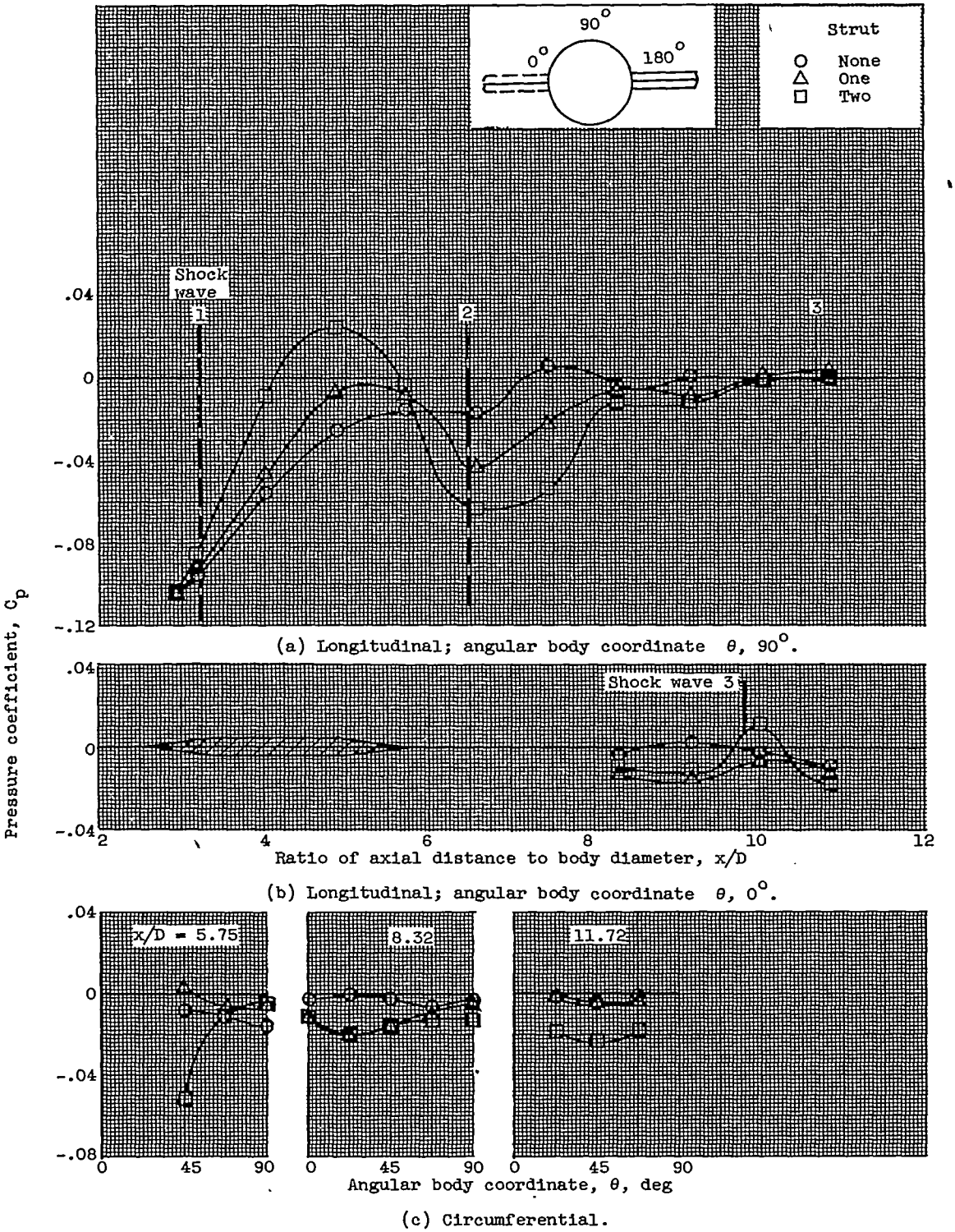

(c) Circumferential.

Figure 5. - Experimental body-pressure distributions for strut C (thickness ratio, 0.070; wedge half-angle, 8°).

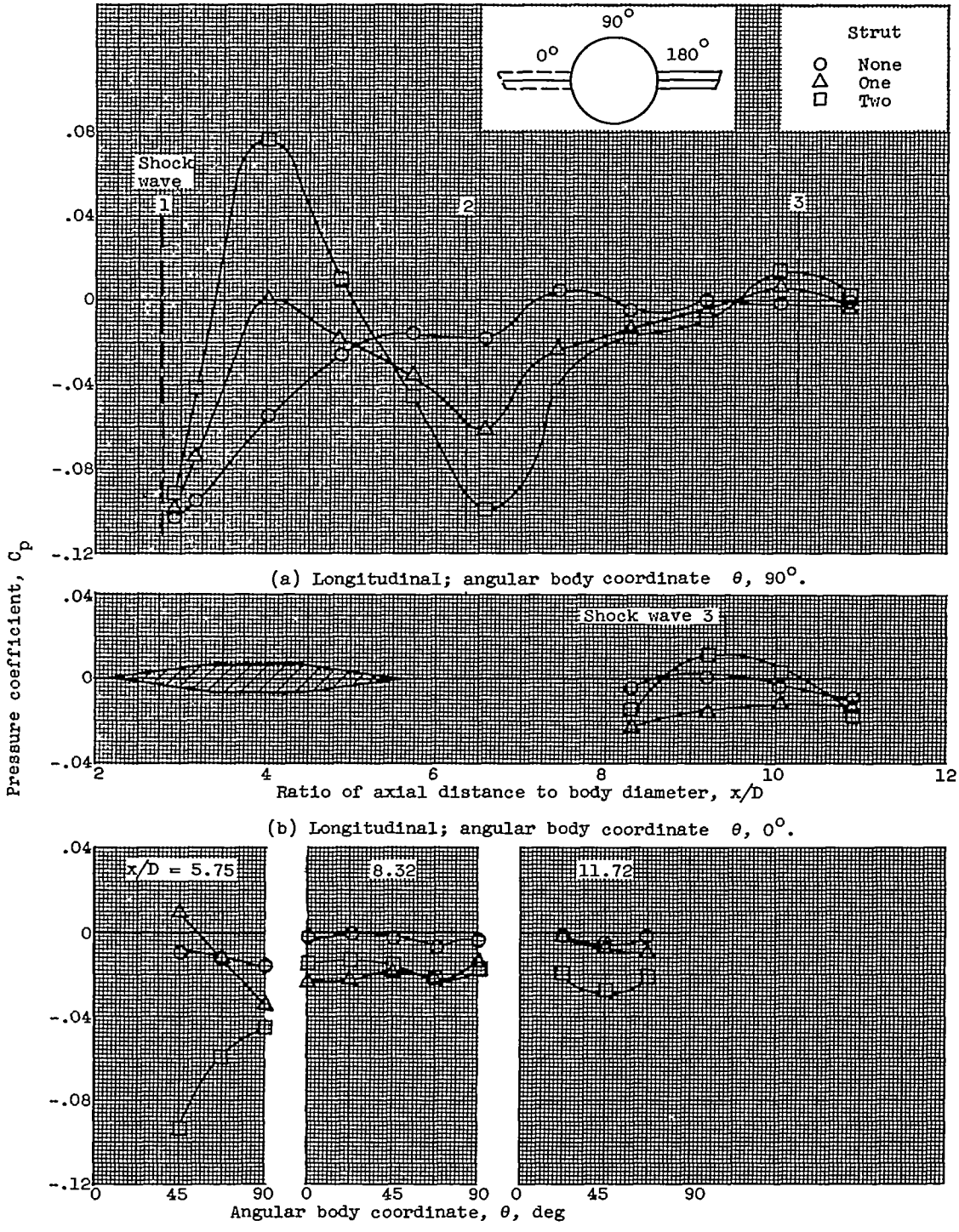

(a) Longitudinal; angular body coordinate θ, 90°.

(b) Longitudinal; angular body coordinate θ, 0°.

(c) Circumferential.

Figure 6. - Experimental body-pressure distributions for strut D (thickness ratio, 0.100; wedge half-angle, 8°).

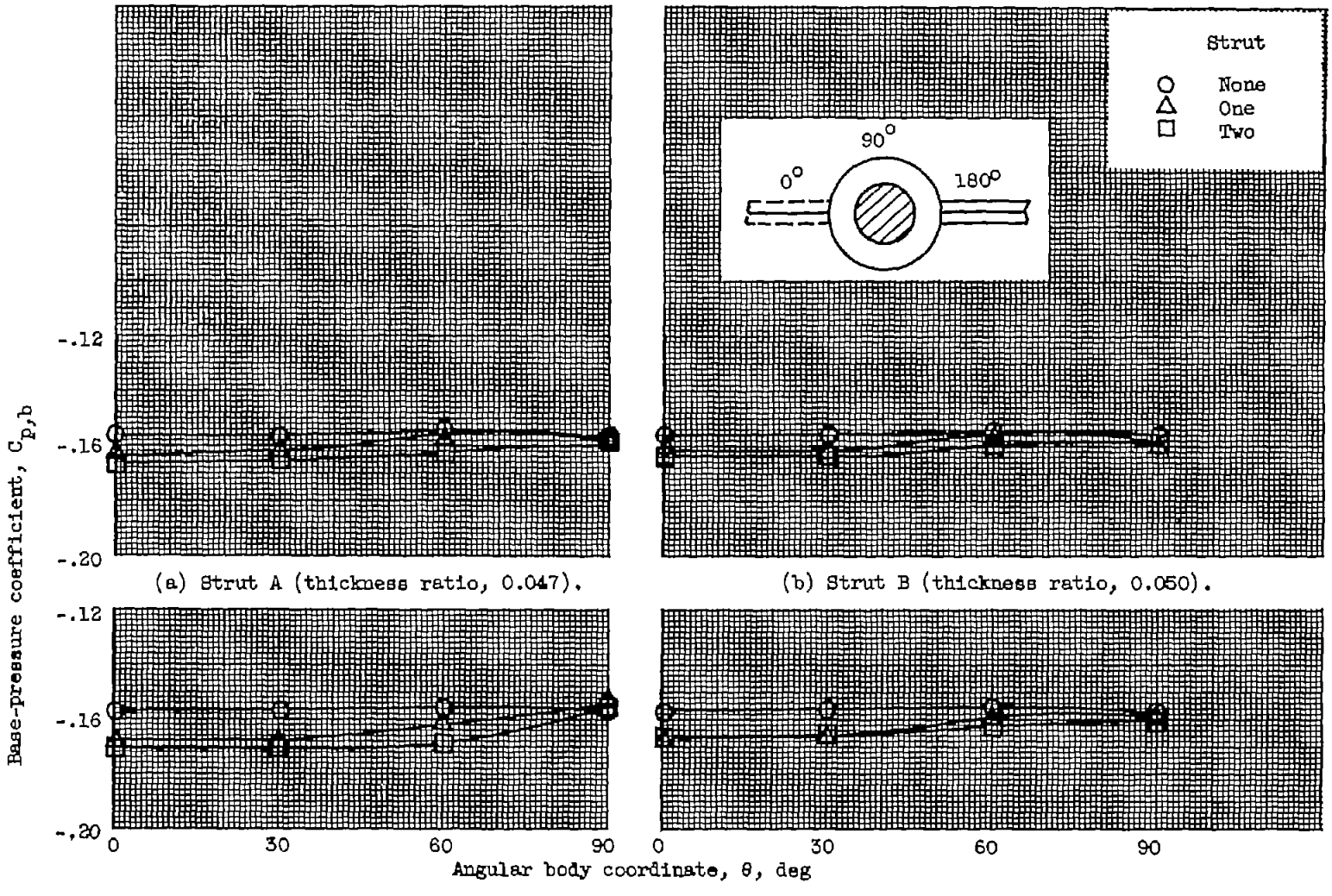

(a) Strut A (thickness ratio, 0.047).

(b) Strut B (thickness ratio, 0.050).

(c) Strut C (thickness ratio, 0.070).

(d) Strut D (thickness ratio, 0.100).

Figure 7. - Body base-pressure distributions.

NACA - Langley Field, Va.